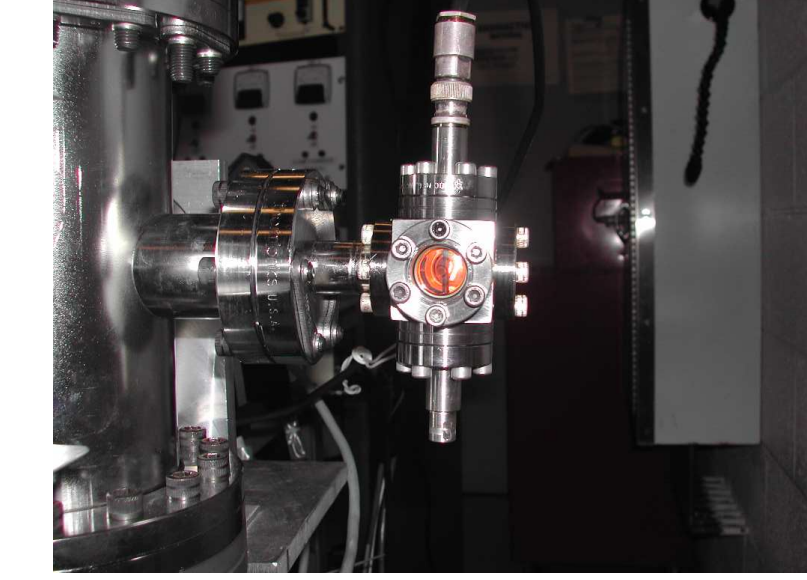


Windowless Far-Ultraviolet Electron Impact Calibration Lamp

Kevin France, Stephan R. McCandliss, and Russell Pelton (JHU)



Abstract

We present preliminary results from a windowless calibration lamp for determining wavelength solutions and detector flat-fielding at far-ultraviolet wavelengths. This lamp produces free electrons from a filament, accelerating them toward a tungsten target by an applied voltage ($\approx 200 - 2000$ V). An emission line spectrum is produced by electrons impacting the residual gas molecules present and continuous emission is produced by bremsstrahlung as the electrons collide with the target. The emission line spectrum can be modified to provide a rich wavelength coverage by introducing different species, and spectra of H_2 , HD, Ar, N_2 , O_2 , and CO_2 have been measured at modest spectral resolution (≈ 1 Å) across the far-UV bandpass (900 – 1400 Å). The long wavelength tail of the x-ray bremsstrahlung continuum falling in this bandpass can be used to make detector flat-field measurements. The lamp is robust and compact, housed in a mini-conflat cube and operates at the ambient vacuum compatible with microchannel plate operation. It is scheduled to be tested on an upcoming sounding rocket flight. We present initial results of both electron impact and bremsstrahlung spectra and adaptability to space-based instrumentation.

Lamp Mechanical Structure and Emission Characteristics

Introduction Astronomers have long relied on emission line and continuum calibration spectra to improve science return at optical wavelengths. Emission line spectra provide wavelength solutions and continuum spectra allow for the construction of detector flat-field maps that can be used to correct for instrumental non-uniformities during the data reduction process. The most common method of obtaining such spectra is through the use of lamps designed for each process. Calibration spectra in the windowless ultraviolet are challenging to obtain as emission line sources generally require operating pressures of ≈ 1 Torr (McCandliss et al. 2000), several orders of magnitude higher than the operating pressure ($\approx 10^{-5}$ Torr) of micro-channel plate (MCP) detectors commonly used in the far-ultraviolet (FUV) bandpass. Continuum sources are even harder to come by as most continuum sources are dominated by line emission. We report on the development of a lamp that serves as both an emission line and continuum source, and operates at the ambient vacuum necessary for FUV instrumentation.

Lamp Mechanical Structure and Operation We have found that electron impact sources can produce strong FUV emission line and continuum spectra in high vacuum environments ($\geq 10^{-7}$ Torr). The line spectrum is produced as free electrons collide with the residual gas in the vacuum. The continuum spectrum is produced by bremsstrahlung as the electrons collide with a thick tungsten target (Bayard and Alpert 1950). In practice, current flowing through a thin tungsten ribbon filament produces a source of free electrons that are accelerated towards the target by an applied voltage. The filament is typically run at 3 – 4 Amps, and tests have been performed with target biases ranging from 20 – 2000 Volts. Unlike traditional electron impact experiments (Ajello et al. 1991; James et al. 1997), the geometry of our lamp does not produce a mono-energetic environment. Our results indicate that our lamp approximates previous mono-energetic experiments when dividing our operating voltage by a factor between four and five.

The lamp consists of a mini-cff cube into which are mounted the filament in proximity to the tungsten target, a $3/32$ " diameter rod. The lamp has a window for visual inspection and filament temperature determination during operation. In the current test configuration, the lamp directly illuminates the slit jaw of a long-slit Rowland Circle spectrograph that was the primary science instrument on three previous sounding rocket flights (NASA/JHU 36.136, 36.186, and 36.198, see Burgh et al. 2002). The spectrograph aperture is a narrow slit ($25 \mu m$), and uses a holographically ruled grating and MCP stack detector with a KBr photocathode, readout by a double-delay line anode. All data presented here were obtained in this configuration with a spectral resolution of about 1 Å.

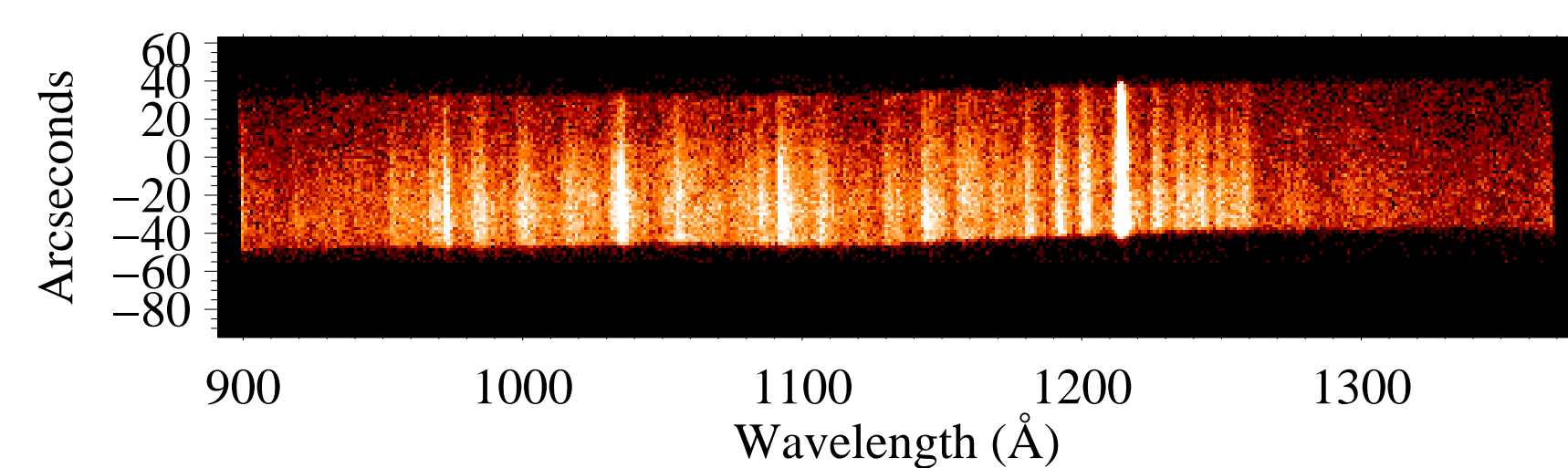


Figure 1. Raw spectral image of electron impact on HD. Gas leaked into the testbed raised the pressure to 4.5×10^{-6} Torr, and the emission spectrum is seen superimposed over the continuum.

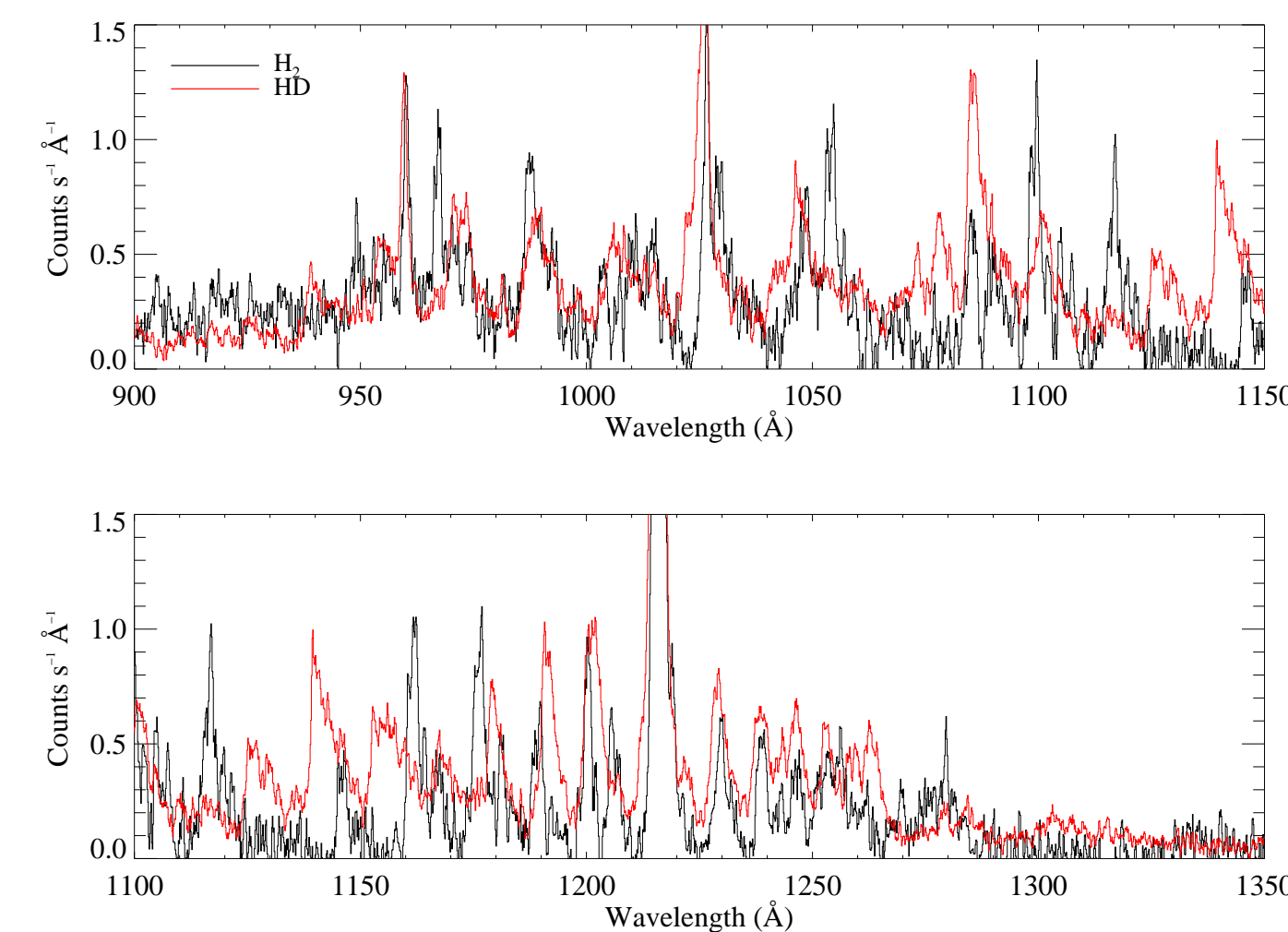


Figure 2. A comparison of the electron impact induced spectra of H_2 and HD, with a target bias of 1.2 kV. The HD spectrum, plotted in red, shows a band structure that differs from H_2 due to the different term values and oscillator strengths of HD.

Emission Characteristics A typical emission line spectrum shows atomic hydrogen, atomic and molecular nitrogen, and atomic oxygen; a combination of atmospheric constituents and water vapor. The spectrum can be altered by the introduction of different species into the lamp. The emission lines present and their strength will depend on the gas and the quality of the vacuum. A gas leak valve on our testbed allows us to introduce different species for a richer wavelength coverage and absolute calibration studies using electron impact cross-sections, as described below. To date, electron impact spectra of H_2 , HD, Ar, N_2 , O_2 , and CO_2 have been measured. Typically lines of H I Lyman- α , N I $\lambda 1200$, N II $\lambda 1084$, O I $\lambda 1304$, O I $\lambda 989$, and N_2 (c_4^2-X) 958 dominate, while Lyman- β , O I $\lambda 1152$, N I $\lambda 1243$, N I $\lambda 1135$, C II $\lambda 1335$, CO (B-X) 1150 and CO (C-X) 1088 are weaker. A comparison of the band structure of H_2 and HD is presented in Figure 2.

The bremsstrahlung continuum spectrum is a strong function of electron emission current (ie- filament temperature) and target voltage. Emission current increases sharply as the filament temperature goes above > 1100 K. The dependence on operating pressure is much weaker than in the case of the emission lines, thus continuum/line contrast can be varied by changing the lamp pressure. This contrast can also be changed by increasing the target bias (see Figure 3). The bremsstrahlung emission rises with bias where the expected cross-sections for impact excitation of molecules typically rise to a peak at 50 – 100 eV and then fall towards higher electron energies (Ajello et al. 1989; Ajello et al. 1991; James et al. 1997; Kanik et al. 1995; and Shemansky et al. 1985). Our source follows this trend even though the energy of electrons in the line emitting volume is not mono-energetic.

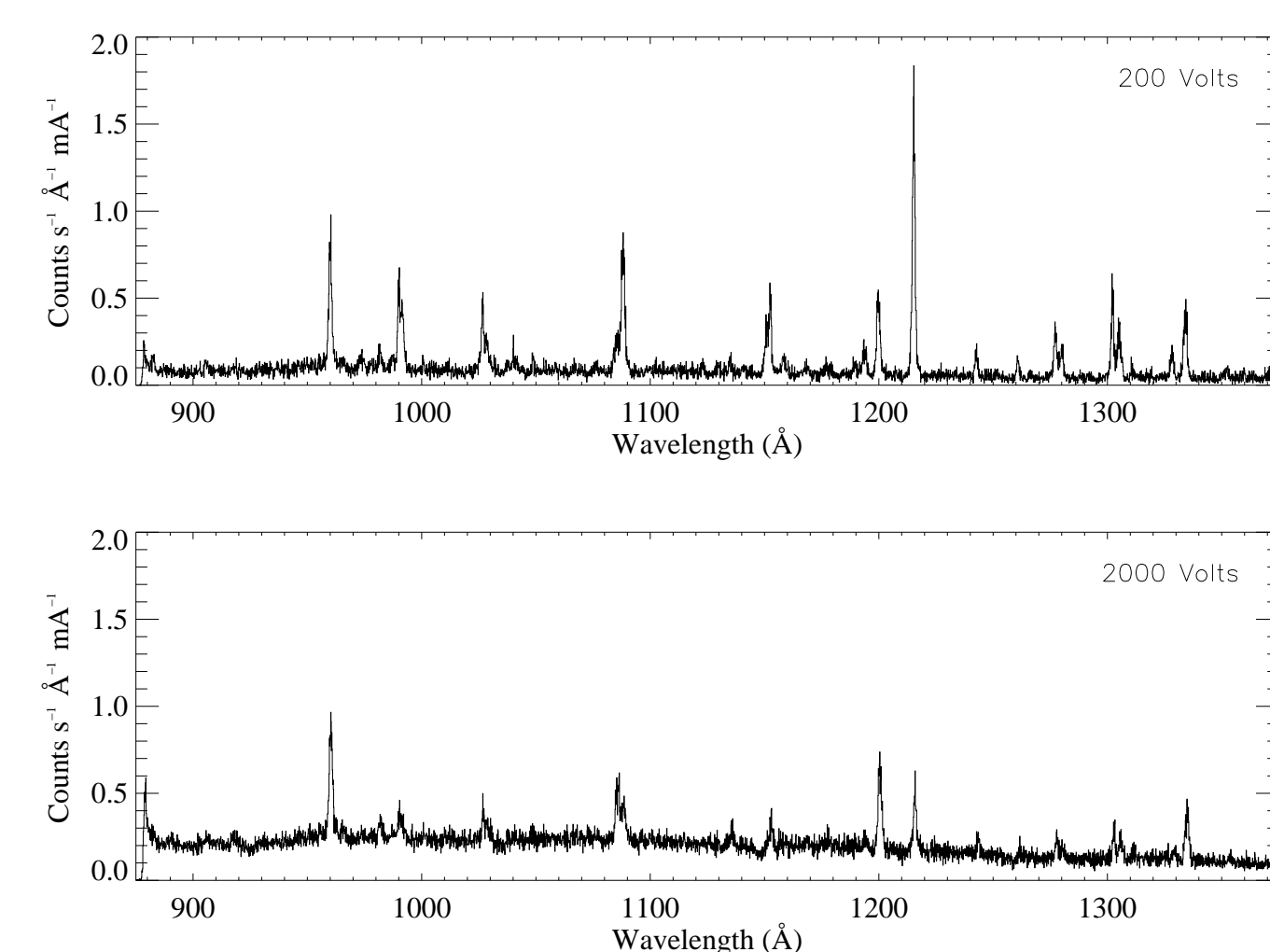


Figure 3. The emission line to continuum ratio decreases at higher target voltages. The spectra shown here are bremsstrahlung and electron impact on CO_2 with target voltages of 200 and 2000 Volts.

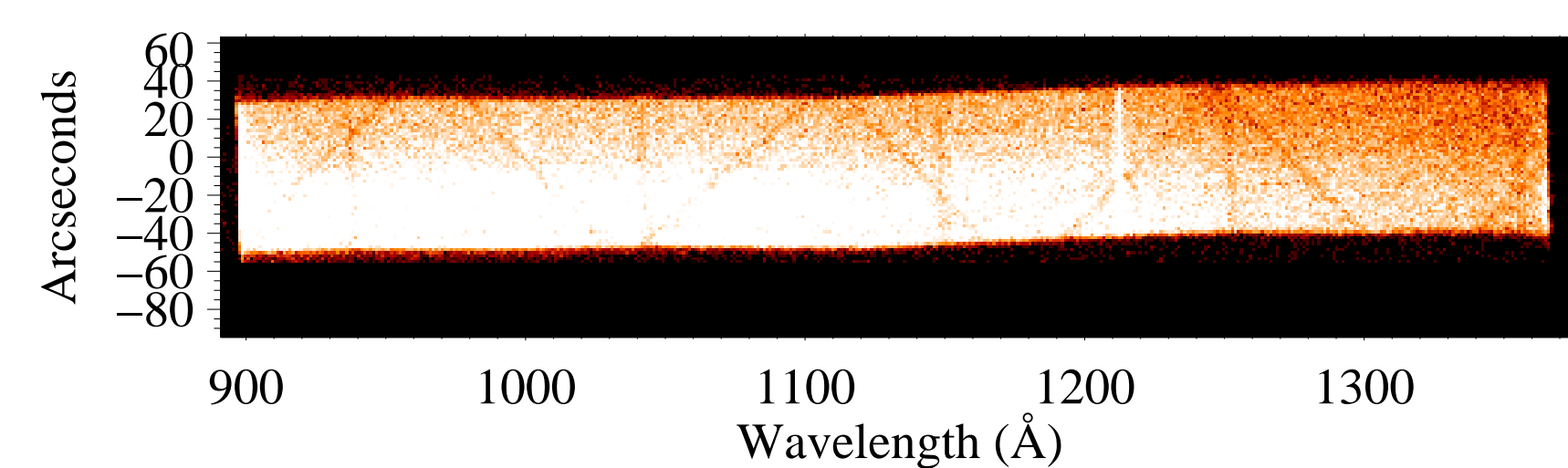


Figure 4. Raw spectral image of bremsstrahlung continuum at the testbed baseline pressure of 3×10^{-8} Torr. The brightness gradient across the images is due to vignetting within the spectrograph.

Impact Cross-Sections and Absolute Calibration

We have found the rise and fall of our Lyman- α intensity to span a much wider range of target voltage than found in the Ajello work where mono-energetic electrons were used. Our understanding of this discrepancy has been aided by the development of a n-body code to calculate the trajectories of the electrons emitted by the lamp filament and attracted towards the target rod. This code allows us to determine the electron energy distribution within the line emitting region. We found that the average energy of the electrons was ≈ 4.5 of the maximum provided by the target voltage, in good agreement with the expanded energy scale in comparison with Ajello's data. The scale change allowed a much closer match to Ajello's work, and we are now addressing discrepancies associated with the non-mono-energetic electron distribution.

For gas species with known measured cross-sections, an absolute flux can be predicted using these known values as well as a knowledge of the individual species density, electron flux, and the geometry of impact region (James et al. 1997). The electron flux can be measured from the electron emission current, thus, absolute calibration will require two additional quantities, the partial pressure of the emitting species and a detailed understanding of the emitting volume. The partial pressures can be provided by a residual gas analyzer. The emitting volume will come from the n-body calculations.

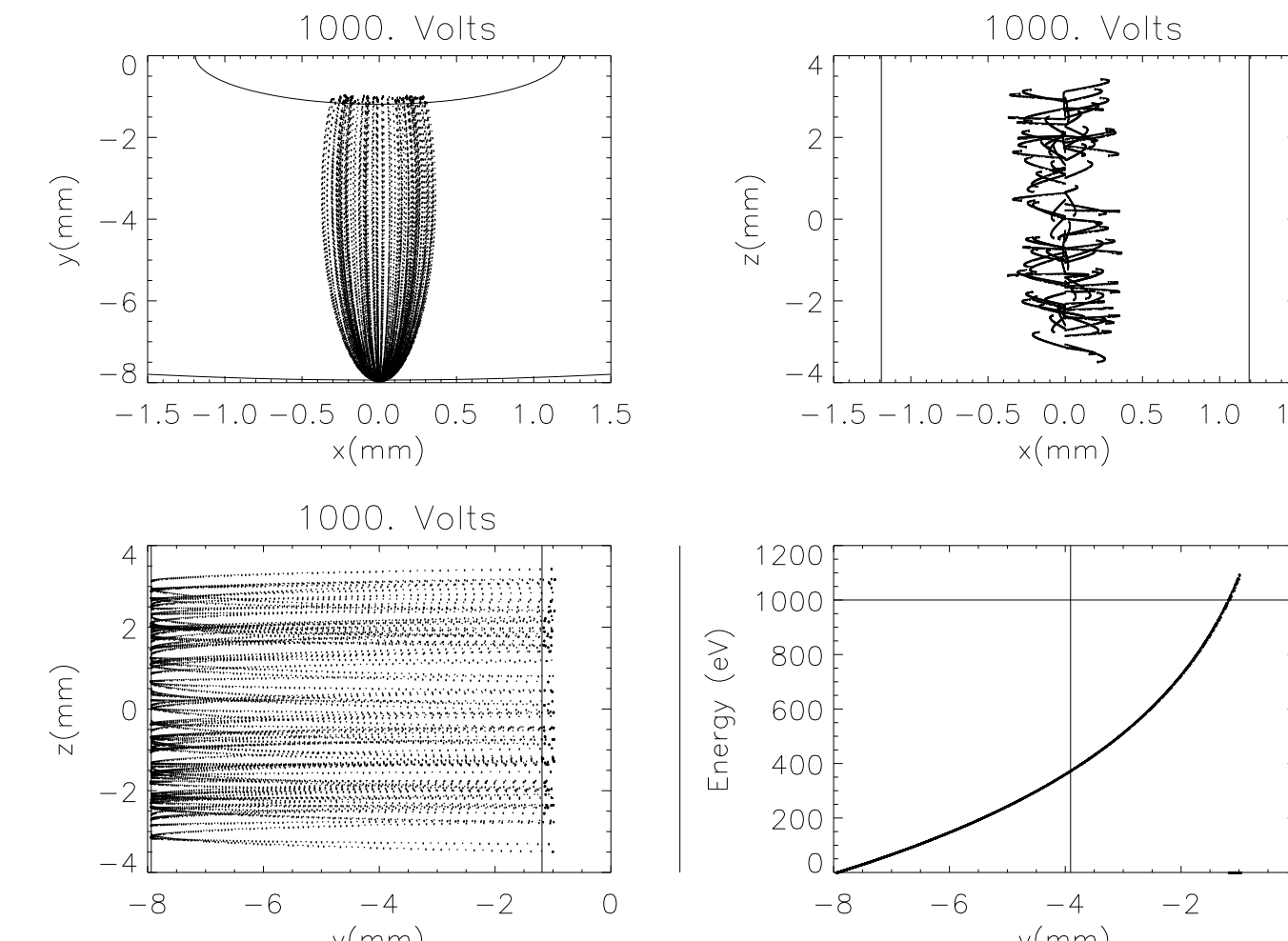


Figure 5. N-body simulation of the electron distribution between the filament and the target for a target voltage of 1000 V. Increasing the target voltage results in a tighter spatial distribution as well as a narrower distribution in the relative electron energies.

The extensive set of gas species and energies measured thus far provides data for theoretical calculations seeking to reproduce the emission line intensity variation produced by the integrated distribution of electron energies inherent to the lamp filament-target geometry, a task critical to the development of an absolute calibration. If it is found that we can predict and verify the emission line intensities of a variety of gases and we find that they are repeatable from lamp to lamp, then we can transfer these emission line calibrations to the continuum emission at select wavelengths. We know that the spectral energy distribution of the bremsstrahlung continuum is a slowly varying powerlaw in our wavelength range (Stephenson and Mason 1949) so the transfer of emission line calibrations will in effect provide a means for a self calibrated primary standard at all wavelengths in the bandpass.

To date we have used the current configuration to study the relative calibration offered by the stability and reproducibility of the continuum shape in this bandpass (see Figure 6). In these experiments the continuum slope was found to flatten as the target voltage increased, in agreement with the expectations for bremsstrahlung emission. At high target voltage and direct illumination of the spectrograph slit, the spectrum of the continuum closely follows the shape of the absolute calibration curve of the spectrograph to within an arbitrary scale factor. The match is so close that where it does differ we are beginning to question the accuracy of the absolute calibration.

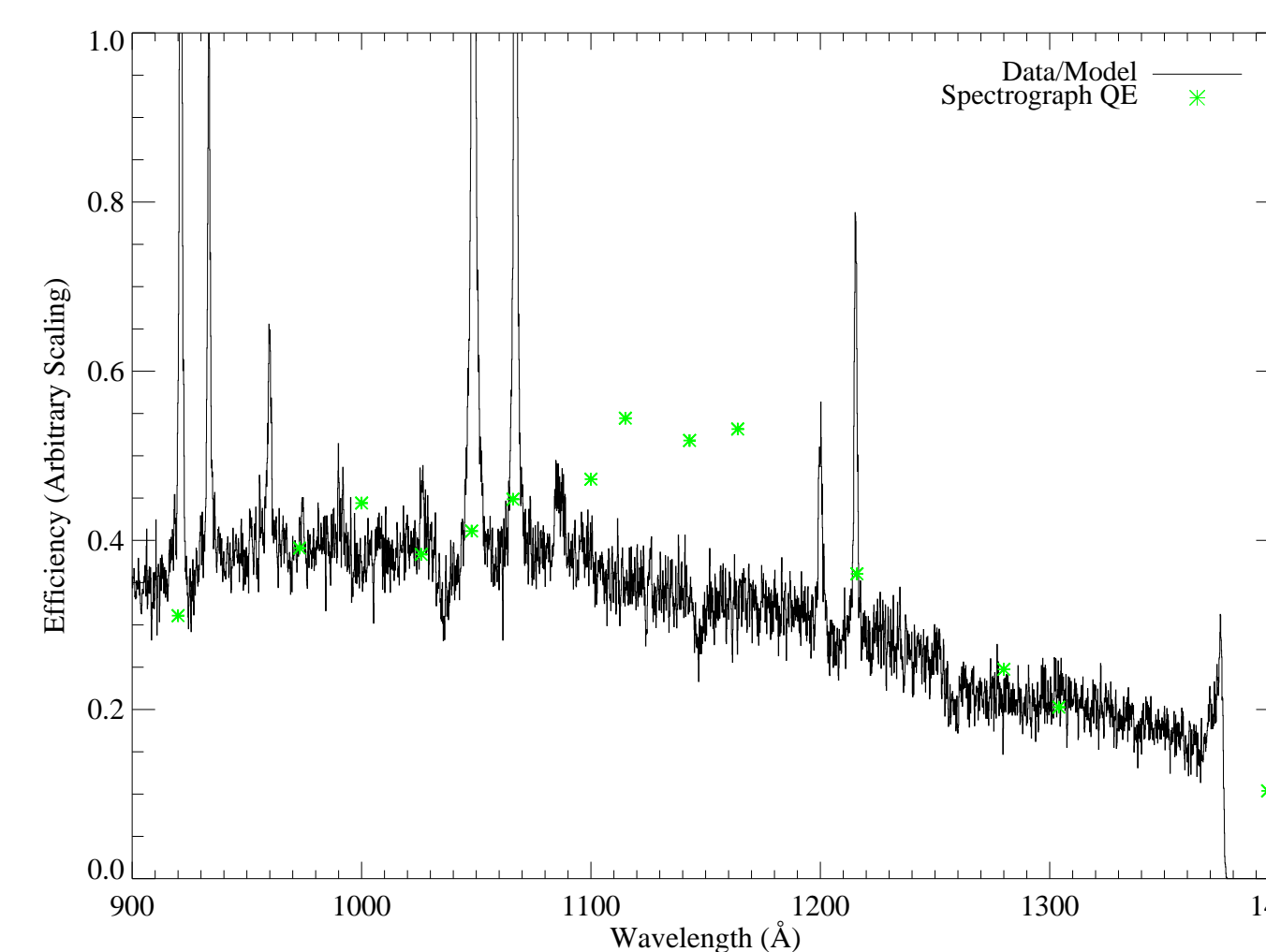


Figure 6. A comparison of the independently measured efficiency of our current spectrograph and a lamp spectrum taken with a target bias of 1.2 kV. The electron impact induced emission lines (Argon) provide a wavelength calibration, and dividing out a thick-target bremsstrahlung continuum model roughly reproduces the spectrograph efficiency.

Electron Impact Lamp for In-Flight Calibration

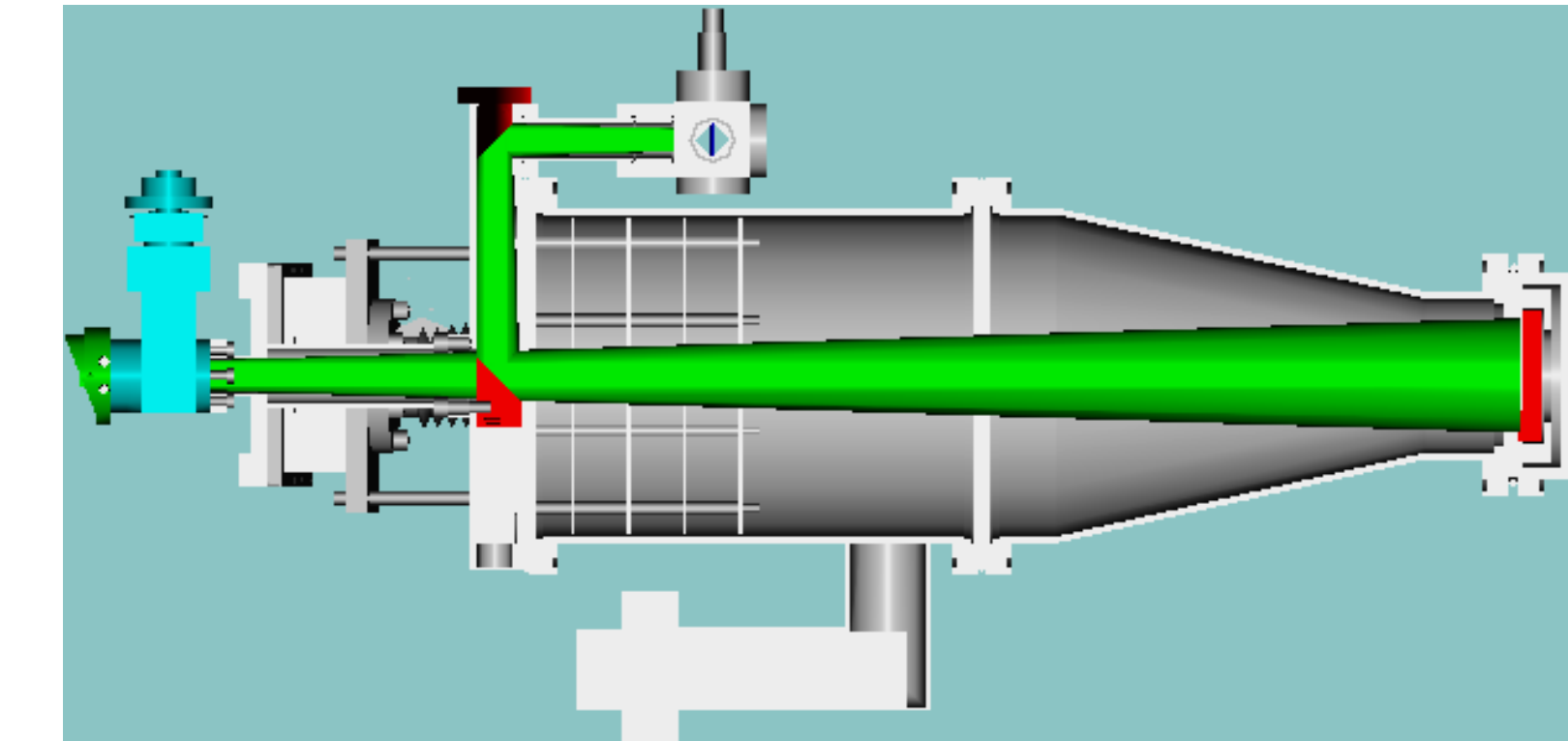


Figure 7. Cutaway shows the optical path of the electron impact calibration lamp and the telescope input in green. The tungsten target is shown in blue. The pickoff flats and gratings are shown in red.

Figure 7 shows the calibration lamp integrated into the optical path of the Long-Slit Imaging Dual Order Spectrograph (LIDOS), currently under development by the JHU Sounding Rocket Group (McCandliss et al. 2002). An entrance slit for the lamp is mounted in the copper gasket in the flange joining the lamp to the spectrograph. A deep channel running the diameter of the baseplate allows for the propagation of a beam from the lamp slit into an optical path intercepting the grating and detectors. Both mirrors are made from polished stainless steel and overcoated with ion beam sputtered SiC. The first is a simple 45° elliptical flat. The second, located along the telescope optical axis, has a horseshoe shaped cutout to allow an unobstructed passage of the telescope beam, while picking off the faster calibration beam and redirecting it towards the grating.

LIDOS is designed to observe UV-bright objects and their fainter surrounding nebosity simultaneously in the FUV bandpass (900 – 1650 Å) at moderate spectral (≈ 3 Å) and spatial ($\approx 3''$) resolution. LIDOS uses complementary detectors to cover a large dynamic range in a single observation. Bright objects are observed with a δ -doped charge coupled device, whose high maximum count rate (corresponding to objects with UV fluxes $F_{UV} \leq 10^{-7}$ ergs $s^{-1} cm^{-2} \text{Å}^{-1}$) will allow measurements of stars several orders of magnitude beyond the bright limit of instruments such as FUSE. Faint extended emission is observed with a MCP channel that employs a coronagraphic strip to occult the bright central object. The MCP channel takes advantage of the low background equivalent flux of such a detector and extends the LIDOS faint limit to fluxes of $F_{UV} \leq \text{few} \times 10^{-14}$ ergs $s^{-1} cm^{-2} \text{Å}^{-1}$ for a signal-to-noise ratio of 3 over typical sounding rocket integration times. The electron impact calibration lamp shares a common vacuum with the detectors and will be used in all phases of integration and testing. In-flight, the lamp will be turned on via a timer event and will provide realtime wavelength and flat-field calibration during the science acquisition.

Future Work

Fabrication of the final flight version of the calibration lamp is underway. The compact and rugged design of the lamp is inherently robust, appropriate to the high-stress environments of a space-based mission. Further work will be required in designing a wiring harness for the lamp that is more sturdy than the current laboratory configuration and can be integrated into the payload power system. We anticipate a first flight for LIDOS in August-September 2003. A complete model of the internal lamp environment will bring us closer to using this lamp as an absolute calibration source. The full characterization of the lamp as an absolute calibration source would drastically reduce the time and effort that goes into the pre and post-flight calibration processes, allowing for a faster turn around between flights, hence, an enhanced science return. Such a source could also be of similar use to the general ultraviolet astronomy community.

This work was supported by NASA grant NAG5-5315 to The Johns Hopkins University.

REFERENCES

- Ajello, J. M., James, G. K., Franklin, B. O., & Shemansky, D. E. 1989, *Phys. Rev. A*, 40, 3524–3556.
- Ajello, J. M., James, G. K., & Shemansky, D. E. 1991, *ApJ*, 371, 422–431.
- Bayard, R. T. & Alpert, D. 1950, *Rev. Sci. Instr.*, 21, 571.
- Burgh, E. B., McCandliss, S. R., & Feldman, P. D. 2002, *ApJ*, 575, 240–249.
- James, G. K., Slevin, J. A., Shemansky, D. E., McConkey, J. W., Bray, I., Dziczek, D., Kanik, I., & Ajello, J. M. 1997, *Phys. Rev. A*, 55, 1069–1087.
- Kanik, I., James, G. K., & Ajello, J. M. 1995, *Phys. Rev. A*, 51, 2067–2074.
- McCandliss, S. R., Burgh, E. B., & Feldman, P. D. 2000, In *Proceedings of the SPIE*, Volume 4139.
- McCandliss, S. R., France, K., Feldman, P. D., & Pelton, R. 2002, In *Proceedings of the SPIE*, Volume 4854.
- Shemansky, D. E., Hall, D. T., & Ajello, J. M. 1985, *ApJ*, 296, 765–773.
- Stephenson, S. T. & Mason, F. D. 1949, *Phys. Rev.*, 11, 1711–1716.

Fig. 1.—

Fig. 2.—

Fig. 3.—

Fig. 4.—

Fig. 5.—

Fig. 6.—

Fig. 7.—